HHS Public Access

Author manuscript

Drug Deliv Transl Res. Author manuscript; available in PMC 2017 July 13.

Published in final edited form as:

Drug Deliv Transl Res. 2016 June ; 6(3): 225–233. doi:10.1007/s13346-016-0294-y.

Liposome size and charge optimization for intraarterial delivery to gliomas

Shailendra Joshi, M.D.[1], **Johann R. N. Cooke, M.S.**[1], **Darren K. W. Chan, M.S.**[2], **Jason A. Ellis, M.D.**[3], **Shaolie S. Hossain, Ph.D.**[4,5], **Rajinder P. Singh-Moon, B.S.**[6], **Mei Wang, M.S.**[1], **Irving J. Bigio, Ph.D.**[7], **Jeffrey N. Bruce, M.D.**[3], and **Robert M. Straubinger, Ph.D.**[2,8]

[1]Department of Anesthesiology, Columbia University Medical Center, New York, NY

[2]Department of Pharmaceutical Sciences, State University of New York at Buffalo, NY

[3]Department of Neurological Surgery, Columbia University Medical Center, New York, NY

[4]Department of Molecular Cardiology, Texas Heart Institute, Houston, TX

[5]Institute for Computational Engineering and Sciences, University of Texas at Austin, TX

[6]Department of Electrical Engineering, Columbia University, New York, NY

[7]Department of Electrical Engineering and Biomedical Engineering, Boston University, Boston, MA

[8]Department of Pharmacology and Therapeutics, Roswell Park Cancer Institute, Buffalo, NY

Abstract

Nanoparticles such as liposomes may be used as drug delivery vehicles for brain tumor therapy. Particle geometry and electrostatic properties have been hypothesized to be important determinants of effective tumor targeting after intraarterial injection. In this study we investigate the combined roles of liposome size and surface charge on the effectiveness of delivery to gliomas after intraarterial injection. Intracarotid injection of liposomes was performed in separate cohorts of both healthy and C6 glioma-bearing Sprague Dawley rats after induction of transient cerebral hypoperfusion. Large (200 nm) and small (60–80 nm) fluorescent dye-loaded liposomes that were either cationic or neutral in surface charge were utilized. Delivery effectiveness was quantitatively measured both with real-time, in vivo and post-mortem diffuse reflectance spectroscopy. Semi-quantitative multispectral fluorescence imaging was also utilized to assess the pattern and extent of liposome targeting within tumors. Large cationic liposomes demonstrated the most effective hemispheric and glioma targeting of all the liposomes tested. Selective large cationic liposome retention at the site of glioma growth was observed. The liposome deposition pattern within

Corresponding Author: Shailendra Joshi, M.D., Department of Anesthesiology, Columbia University Medical Center, 630 West 168th Street, P&S Box 46, New York, NY 10032, Ph: 212 305 0021, Fax: 212 305 8287, sj121@cumc.columbia.edu.

Ethical Standards

All experiments reported comply with the current laws of the United States of America. All experiments were approved by the Columbia University Institutional Review Board and the Animal Care and Use Committee.

Disclosures

Shailendra Joshi, Johann R. N. Cooke, Darren K. W. Chan, Jason A. Ellis, Shaolie S. Hossain, Rajinder P. Singh-Moon, Mei Wang, Irving J. Bigio, Jeffrey N. Bruce, and Robert M. Straubinger declare that they have no conflict of interest.

tumors after intraarterial injection was variable with both core penetration and peripheral deposition observed in specific tumors. This study provides evidence that liposome size and charge are important determinants of effective brain and glioma targeting after intraarterial injection. Our results support the future development of 200 nm cationic liposomal formulations of candidate intraarterial anti-glioma agents for further pre-clinical testing.

Keywords

brain tumor; chemotherapy; glioblastoma; nanoparticle

Introduction

Selective intraarterial (IA) nanoparticle delivery could provide a vehicle for the delivery of a broad range of brain tumor therapeutic agents.[1, 2] However, the pharmacokinetics of such a strategy are complex and not well-understood.[3, 4] In theory, the regional deposition of nanoparticles after IA injection reflects a balance between the forces promoting attachment to the vascular endothelium and the hydrodynamic and sheer stress that tends to displace them (Figure 1).[5–7] For spherical nanoparticles such as liposomes, computational models suggest that the force of attachment largely depends on size and surface charge characteristics.[7]

Although preliminary experiments indicate that cationic charge may improve tissue deposition of liposomes after IA injection, the combined roles of particle size and charge remain unclear.[3, 8, 9] Furthermore, the hemodynamic consequences of altering these particle characteristics have not been rigorously studied in animal glioma models. In the present study we investigate the combined effect of liposome size and charge on delivery efficiency after IA injection. Utilizing the well-established method of IA injection during transient cerebral hypoperfusion (TCH) we demonstrate that both the ipsilateral brain hemisphere and, more specifically, glioma tissue are preferentially targeted by cationic liposomes in a size-dependent manner.

Methods

General

All experiments were approved by the Columbia University Institutional Review Board and the Animal Care and Use Committee. Details of animal care and monitoring, anesthetic protocol, C-6 glioma culture and stereotactic implantation, and induction of transient cerebral hypoperfusion (TCH) can be found in our prior publications.[9, 4, 8] Four experimental groups consisting of 7 animals each included cohorts injected with: 1. small neutral liposomes, 2. large neutral liposomes, 3. small cationic liposomes, and 4. large cationic liposomes. Experiments were replicated in both glioma-bearing and non-glioma bearing animals. Gliomas were allowed to grow for 1 week in vivo prior to the start of experiments in order to ensure relatively small tumor sizes and no animal morbidity. Small liposomes were defined as those having a diameter of 60–80 nm and large liposomes were defined as those having a diameter of 200 nm.

Animal preparation

Sprague Dawley rats were utilized for all animal experiments. Anesthesia was induced with 5% isoflurane and intramuscular ketamine. The internal carotid artery was surgically isolated while other branches of the common carotid artery were ligated to ensure selective delivery to the ipsilateral brain hemisphere. The common carotid artery was cannulated using polyethylene P-50 tubing. Animals were then placed on a stereotactic frame for scalp incision and calvarial drilling. The skull was exposed and the parietal bone was thinned to near transparency over the middle cerebral artery distribution. The frontal bone was also prepared in a similar manner for placement of a laser Doppler probe to record changes in cerebral blood flow. The fiber optic probe for diffuse reflectance spectroscopy (DRS) was placed over the parietal region. Physiological parameters were monitored including electrocardiogram, mean arterial pressure, inspired and expired oxygen, carbon-dioxide and isoflurane concentrations, respiratory rate, skin blood flow, pulse-oxygen saturation, pulse volume, and rectal temperature.

Liposome Preparation

Dimyristoylphosphatidylcholine (DMPC) and dioleoyl-trimethylammonium-propane (DOTAP) were obtained from Avanti Polar Lipids (Alabaster, AL). Cholesterol (Chol) was obtained from Sigma-Aldrich (St. Louis, MO). DiD ($DilC_{18}(5)$) was obtained from Invitrogen (Carlsbad, CA). Liposomes were prepared by hydration of dried lipid films with NaCl/TRIS (140/10 mM pH 6.8) buffer, followed by freeze-thawing three times, and then sequential extrusion through polycarbonate filters to a final diameter of 80 or 200 nm.[1, 2, 9] Large liposomes were purified further by centrifugation (28,000 g for 20 min). Cationic liposomes were composed of DMPC:DOTAP:Chol:DiD (2.75:2.75:4.5:1.1 mole % each) and charge-neutral liposomes were composed of DMPC:Chol:DiD (5.5:4.5:1.1 mole %).[10] The zeta potentials of DMPC:DOTAP:Chol:DiD and DMPC:Chol:DiD are −9.53 and 3.7 respectively.

Liposome particle size was measured using a Nanobrook Omni instrument (Brookhaven Inc., Holtsville, NY). The charge-neutral liposomes (DMPC:Chol) had mean diameters of 60 or 200 nm, with a polydispersity index (PDI) of 0.236. The cationic liposomes containing 50% DOTAP had mean diameters of 80 or 200 nm (PDI 0.095). The liposome membrane was labeled with a nonexchangeable dialkyl carbocyanine dye $DilC18_{18}(5)$ (DiD) which has peak absorption at 650 nm and emission at 670 nm.[11, 12] The final phospholipid concentration of the liposome preparations was 10 mM for all except the 200 nm cationic liposomes, which was 8.4 mM. Therefore, the injection volume was adjusted to ensure administration of equal lipid doses.

Intraarterial injection

Carotid artery injections consisted of micro-boluses of 50–60 μl using a pneumatic syringe system consisting of a pressure ejector (Picospritzer III, Parker Hannifin, Pine Brook, NJ) controlled by a signal generator (Model #33220A Agilent Technologies Inc. Santa Clara, CA). Typically, 15 injections were needed to ensure delivery of the liposome volume.

Spectroscopy and fluorescence imaging

Diffuse reflectance spectroscopy (DRS) measurements were obtained using a custom-built spectroscope (Optimum Technologies Inc., Southbridge, MA) to measure the concentration of membrane-incorporated DiD dye.[13] In all, 612 measurements of tissue concentrations were made over a 45-minute period for in vivo samples. The pharmacokinetic parameters recorded were peak concentration, end concentration, and the total area under the concentration-time curve (AUC). Single time point, post-mortem DRS was also performed in tumor tissue.

Multispectral imaging (MSI) was used to determine the liposome distribution in postmortem tissue samples. Measurements were obtained on whole brain and on coronal sections using 635±5 nm LED light excitation, while imaging through a 680± 5 nm band-pass filter using a CCD camera (Allied Vision Technology Prosilica CE camera).[4]

Statistical analysis

Statistical analysis was performed using Stat View 5.2 (SAS Institute, Cary NC). Data were analyzed using ANOVA and factorial ANOVA. Post-hoc corrections (Bonferroni-Dunn) were performed when multiple comparisons were made. Statistical significance was set at $p<0.05$.

Results

Physiological and hemodynamic analysis during liposome injection

Physiological and hemodynamic parameters were measured in healthy rats during IA injections to test for liposome-related changes in blood flow. All experimental groups showed a similar pattern and degree of hemodynamic change during transient cerebral hypoperfusion (TCH) suggesting uniform IA delivery physiology (Figure 2). No differences in the severity of hypotension or in the degree of cerebral blood flow reduction during injection were seen. Trends suggesting faster recovery of blood flow with large neutral liposome delivery and slower recovery with large cationic liposome delivery were observed but not shown to be significant. No evidence of prolonged cerebral blood flow stagnation or occlusion was observed during delivery of liposomes of any size.

Liposome deposition in normal brain

In vivo DRS measurements indicate that of all experimental groups, large cationic liposomes are most effectively delivered to the hemisphere ipsilateral to carotid artery injection. Although measured peak concentrations were highest for cationic liposome formulations, this was not statistically significant, reflecting that at this early time-point the bulk of signal is contributed by liposomes in the blood space that are not tissue-bound. In contrast, the end concentrations which represent tissue-bound liposomes having a delayed clearance and the overall tissue exposure (area under curve, AUC) were both size and charge dependent with large cationic liposomes having the highest concentrations ($p<0.05$) (Figure 2). Semi-quantitative post-mortem MSI of harvested brains was consistent with the real-time in vivo findings (Figure 3).

Liposome deposition in brain tumors

DRS and MSI revealed no significant uptake of neutral liposomes by the ipsilateral brain hemisphere or glioma tissue. Due to this very low deposition no further testing was done with neutral liposome formulations in tumor-bearing animals. On the other hand, cationic liposomes demonstrated robust targeting to the ipsilateral hemisphere and to the site of tumor growth (Figure 4–5). Delivery efficiency was also seen to be size dependent with large cationic liposomes having increased hemispheric and tumor targeting as compared to small cationic liposomes as quantitated by post-mortem DRS ($p=0.03$). Of note, real-time in vivo DRS concentration measurements did not reveal a significant difference in the delivery of large versus small cationic liposomes and is likely due to insensitivity of the method for deep tumor measurements.

MSI demonstrated a variable pattern of liposome delivery to the tumor mass (Figure 6). Qualitative assessment suggests that tumor core penetration by liposomes becomes less robust and less consistent as the target glioma increases in volume.

Discussion

Liposomes and other nanoparticles can serve as carrier vehicles for targeted delivery to the brain.[2, 14–20] Novel delivery approaches such as intraarterial (IA) administration with the use of transient cerebral hypoperfusion can increase the selectivity of particle delivery in pathological settings such as when gliomas are present.[21, 22, 9, 23, 24] In this study we made three potentially clinically relevant observations including that: 1. varying particle charge and size within the tested range do not appreciably affect cerebral blood flow physiology, 2. cationic liposomal formulations are superior as compared to neutral formulations for brain delivery, and 3. large (200 nm) cationic liposomes are more efficiently targeted to glioma tissue than are smaller (80 nm) cationic liposomes.

Measurement strategy

Our approach to the assessment of IA drug delivery effectiveness presents a number of issues that are worthwhile to discuss. We employ both diffuse reflectance spectroscopy (DRS) and multispectral imaging (MSI) in our analysis of liposome concentrations in brain tissue. The key advantage of DRS is its ability to assess drug/tracer concentrations in a sub-second time frame and to generate site-specific tissue measurements non-invasively.[13] Post-mortem MSI and in some cases DRS can then be used to corroborate calculated deposition concentrations. When employed in such a fashion, DRS and MSI complement each other. Whereas MSI semi-quantitatively interrogates large areas of the tissue sample, DRS provides quantitative drug/tracer concentration measurements in very small volumes of tissues.

A limitation of using DRS for real-time analysis of live tumor-bearing animals is that the method is insensitive to deep subcortical signals. In fact this may entirely explain why our in vivo measurements did not reveal a significant difference in the deposition of large versus small cationic liposomes. Fortunately, concordant post-mortem DRS and MSI indicate that particle size is indeed an important variable that modulates delivery efficiency.

Particle charge

The relative abundance of anionic lipids on cancer endothelia provides a valuable target for cancer detection and treatment strategies, including the delivery of cationic nanoparticles.[25–28] Prior studies have shown that tumor selective uptake of cationic particles is feasible and that cationic particle charge enhances binding to tumor vasculature.[29–32, 17, 33, 34] The microenvironment of the tumor has a considerable effect on drug delivery and these factors in glioma treatment are only recently being investigated.[35, 36]

Anionic lipids are relatively overexpressed in the endothelium of neoplastic tissue, thus imparting a relatively greater negative charge to the neoplastic compared to healthy endothelium.[37] In addition, certain cationic entities are able to penetrate the blood brain barrier through adsorptive transcytosis.[38] Thus, optimizing cationic nanoparticle properties—as we have done through the introduction of size variation—represents an important strategy for developing better intraarterial brain cancer treatments. Indeed, our preliminary observation that liposome deposition is variable and may be dependent on parameters such as tumor volume reinforces that further optimization may be useful.

Particle size

The size of a spherical nanoparticle has two opposing effects on regional deposition. For a particle to stably bind to the vessel wall, the adhesive forces between the cationic particle and the anionic endothelium need to overcome the hydrodynamic stresses that tend to dislodge them. For spherical particles, the larger the particle size the greater the probability of adhesion. This is due to the larger particle surface area being available for adhesive interactions with the vessel wall. However, with increasing particle size, the hydrodynamic drag (dislodging forces) on the particle also increases. This may overwhelm the adhesive forces, making it harder for the particles to stick to the wall. In other words, a large as compared to a small nanoparticle will have a greater surface area of contact with the cerebral vascular endothelium but will be subjected to a greater degree of hydrodynamic stress.

Hossain and coworkers reported this biphasic relationship for a range of particle sizes and demonstrated that the optimum size for maximum adhesion is a function of local hemodynamics.[6] For example, when local hemodynamics are such that wall shear rate is low, the greater the particle size, the more efficiently the particles adhere to the vessel wall. Conversely, when the wall shear rate is high, larger particles adhere less efficiently. Lower wall shear rate promotes particle adhesion as it reduces hydrodynamic stresses while increasing particle residence time, thereby enhancing particle surface-vessel wall (adhesive) interaction. For a given wall shear rate, particle adhesion improves with larger particles until it reaches an optimum (maximum) particle size beyond which particle adhesion becomes less efficient with size increase. This is because the gains in adhesive interactions can no longer overcome the rise in hydrodynamic stresses due to size increase.

Computational analysis suggest that an increase in particle volume to approximately 0.1 μm^3 (576 nm diameter) represents a limit beyond which further size increase is detrimental to particle adhesion.[7] Emerging in vitro studies seem to corroborate these calculations.[5, 6] In the present work, transient cerebral hypoperfusion creates a low wall shear rate

environment that is sustained for a period of time to promote particle adhesion. Under such favorable hydrodynamic conditions, relatively larger liposomes are more effective. This is because gains in adhesive interactions due to the larger area of interaction more than compensates for the corresponding increase in hydrodynamic stresses as a result of size increase.

Particle shape and future studies

Factors that affect the probability of liposome deposition include the number of particles present, shear stress, particle shape and size, and other factors (Figure 1). For example, a computational model by Liu et al. [7] suggests that compared to cylindrical particles of the same volume, spherical particles tend to remain in the center of the stream. The tumbling motion of cylindrical nanoparticles would tend to displace them from an axial flow distribution and also increase the probability of contact with the endothelium. This, in turn, would increase the probability of an elongated particle adhering to the vascular endothelium. Discoid nanoparticles in such simulations also seem better-suited for regional deposition.[7] These modeling concepts are still in early phases of evolution and have been developed to describe particle behavior in large vessels, leaving questions as to what happens at the capillary level, especially during states of hemodynamic instability such as that created by transient arrest of cerebral blood flow. Therefore, application of such modeling approaches to the complex physiological conditions inherent to our experimental model will be important to undertake, so that their limitations can be understood and addressed. The refinement of solid nanoparticles that can be designed to have a variety of shapes in contrast to liposomes is an important future direction for application in the system we present.

Conclusion

This study suggests that cationic liposomes may serve as an effective vehicle for intraarterial delivery to gliomas. We demonstrate that 200 nm cationic liposomes are better retained than 80 nm particles in the brains of both healthy and glioma-bearing animals. Our results support the development of large cationic liposomal formulations of candidate intraarterial anti-glioma agents for further pre-clinical testing.

Acknowledgments

Funding: National Cancer Institute at the National Institutes of Health RO1-CA-138643

References

1. De Baere T, Mariani P. Surgical or percutaneous hepatic artery cannulation for chemotherapy. Journal of visceral surgery. 2014; 151(Suppl 1):S17–S20. [PubMed: 24582544]
2. Drummond DC, Meyer O, Hong K, Kirpotin DB, Papahadjopoulos D. Optimizing liposomes for delivery of chemotherapeutic agents to solid tumors. Pharmacol Rev. 1999; 51(4):691–743. [PubMed: 10581328]
3. Joshi S, Singh-Moon R, Wang M, Bigio IJ. Transient Cerebral Hypoperfusion Assisted Intra-arterial Delivery of Mitoxantrone in C6 Glioma Bearing Rats. Journal of Neurosurgical Anesthesiology. 2014; 26(4):482.
4. Joshi S, Singh-Moon RP, Ellis JA, Chaudhuri DB, Wang M, Reif R, et al. Cerebral hypoperfusion-assisted intra-arterial deposition of liposomes in normal and glioma-bearing rats. Neurosurgery. 2015; 76(1):92–100. [PubMed: 25525695]

5. Hossain SS, Hughes TJ, Decuzzi P. Vascular deposition patterns for nanoparticles in an inflamed patient-specific arterial tree. Biomechanics and modeling in mechanobiology. 2013
6. Hossain SS, Zhang Y, Liang X, Hussain F, Ferrari M, Hughes TJ, et al. In silico vascular modeling for personalized nanoparticle delivery. Nanomedicine. 2013; 8(3):343–357. [PubMed: 23199308]
7. Liu Y, Shah S, Tan J. Computational Modeling of Nanoparticle Targeted Drug Delivery. Reviews in Nanoscience and Nanotechnology. 2012; 1:66–83.
8. Joshi S, Singh-Moon R, Wang M, Chaudhuri DB, Ellis JA, Bruce JN, et al. Cationic surface charge enhances early regional deposition of liposomes after intracarotid injection. Journal of neuro-oncology. 2014
9. Joshi S, Singh-Moon RP, Wang M, Chaudhuri DB, Holcomb M, Straubinger NL, et al. Transient cerebral hypoperfusion assisted intraarterial cationic liposome delivery to brain tissue. Journal of neuro-oncology. 2014
10. Roy Chaudhuri T, Arnold RD, Yang J, Turowski SG, Qu Y, Spernyak JA, et al. Mechanisms of tumor vascular priming by a nanoparticulate doxorubicin formulation. Pharmaceutical research. 2012; 29(12):3312–3324. [PubMed: 22798260]
11. Meers P, Ali S, Erukulla R, Janoff AS. Novel inner monolayer fusion assays reveal differential monolayer mixing associated with cation-dependent membrane fusion. Biochimica et Biophysica Acta. 2000; 1467(1):227–243. [PubMed: 10930525]
12. Saito R, Bringas JR, McKnight TR, Wendland MF, Mamot C, Drummond DC, et al. Distribution of liposomes into brain and rat brain tumor models by convection-enhanced delivery monitored with magnetic resonance imaging. Cancer Res. 2004; 64(7):2572–2579. [PubMed: 15059914]
13. Reif R, Wang M, Joshi S, A'Amar O, Bigio IJ. Optical method for real-time monitoring of drug concentrations facilitates the development of novel methods for drug delivery to brain tissue. J Biomed Opt. 2007; 12(3):034036. [PubMed: 17614744]
14. Arnold RD, Mager DE, Slack JE, Straubinger RM. Effect of repetitive administration of Doxorubicin-containing liposomes on plasma pharmacokinetics and drug biodistribution in a rat brain tumor model. Clin Cancer Res. 2005; 11(24 Pt 1):8856–8865. [PubMed: 16361575]
15. Biswas S, Dodwadkar NS, Deshpande PP, Parab S, Torchilin VP. Surface functionalization of doxorubicin-loaded liposomes with octa-arginine for enhanced anticancer activity. European journal of pharmaceutics and biopharmaceutics : official journal of Arbeitsgemeinschaft fur Pharmazeutische Verfahrenstechnik eV. 2013; 84(3):517–525.
16. Gupta B, Levchenko TS, Torchilin VP. TAT peptide-modified liposomes provide enhanced gene delivery to intracranial human brain tumor xenografts in nude mice. Oncol Res. 2007; 16(8):351–359. [PubMed: 17913043]
17. Zhao M, Chang J, Fu X, Liang C, Liang S, Yan R, et al. Nano-sized cationic polymeric magnetic liposomes significantly improves drug delivery to the brain in rats. J Drug Target. 2012; 20(5): 416–421. [PubMed: 22519867]
18. Zhao H, Li GL, Wang RZ, Li SF, Wei JJ, Feng M, et al. A comparative study of transfection efficiency between liposomes, immunoliposomes and brain-specific immunoliposomes. J Int Med Res. 2010; 38(3):957–966. [PubMed: 20819432]
19. Thole M, Nobmanna S, Huwyler J, Bartmann A, Fricker G. Uptake of cationzied albumin coupled liposomes by cultured porcine brain microvessel endothelial cells and intact brain capillaries. Journal of Drug Targeting. 2002; 10(4):337–344. [PubMed: 12164382]
20. Wen CJ, Zhang LW, Al-Suwayeh SA, Yen TC, Fang JY. Theranostic liposomes loaded with quantum dots and apomorphine for brain targeting and bioimaging. Int J Nanomedicine. 2012; 7:1599–1611. [PubMed: 22619515]
21. Dedrick RL. Arterial drug infusion: pharmacokinetic problems and pitfalls. Journal of the National Cancer Institute. 1988; 80(2):84–89. [PubMed: 3278123]
22. Joshi S, Meyers PM, Ornstein E. Intracarotid delivery of drugs: the potential and the pitfalls. Anesthesiology. 2008; 109(3):543–564. [PubMed: 18719453]
23. Joshi S, Wang M, Etu JJ, Nishanian EV, Pile-Spellman J. Cerebral blood flow affects dose requirements of intracarotid propofol for electrocerebral silence. Anesthesiology. 2006; 104(2): 290–298. [PubMed: 16436848]

24. Joshi S, Wang M, Etu JJ, Suckow RF, Cooper TB, Feinmark SJ, et al. Transient cerebral hypoperfusion enhances intraarterial carmustine deposition into brain tissue. Journal of neuro-oncology. 2007
25. Abercrombie M, Ambrose EJ. The surface properties of cancer cells: a review. Cancer Res. 1962; 22:525–548. [PubMed: 13858936]
26. Dobrzynska I, Skrzydlewska E, Figaszewski ZA. Changes in electric properties of human breast cancer cells. The Journal of membrane biology. 2013; 246(2):161–166. [PubMed: 23135059]
27. Dobrzynska I, Szachowicz-Petelska B, Darewicz B, Figaszewski ZA. Characterization of human bladder cell membrane during cancer transformation. The Journal of membrane biology. 2015; 248(2):301–307. [PubMed: 25572835]
28. Marquez M, Nilsson S, Lennartsson L, Liu Z, Tammela T, Raitanen M, et al. Charge-dependent targeting: results in six tumor cell lines. Anticancer research. 2004; 24(3a):1347–1351. [PubMed: 15274294]
29. Blau S, Jubeh TT, Haupt SM, Rubinstein A. Drug targeting by surface cationization. Crit Rev Ther Drug Carrier Syst. 2000; 17(5):425–465. [PubMed: 11108156]
30. Lu W, Sun Q, Wan J, She Z, Jiang XG. Cationic albumin-conjugated pegylated nanoparticles allow gene delivery into brain tumors via intravenous administration. Cancer Res. 2006; 66(24):11878–11887. [PubMed: 17178885]
31. Lu W, Wan J, Zhang Q, She Z, Jiang X. Aclarubicin-loaded cationic albumin-conjugated pegylated nanoparticle for glioma chemotherapy in rats. Int J Cancer. 2007; 120(2):420–431. [PubMed: 17066446]
32. Mizuno M, Ryuke Y, Yoshida J. Cationic liposomes conjugation to recombinant adenoviral vectors containing herpes simplex virus thymidine kinase gene followed by ganciclovir treatment reduces viral antigenicity and maintains antitumor activity in mouse experimental glioma models. Cancer Gene Ther. 2002; 9(10):825–829. [PubMed: 12224023]
33. Thurston G, McLean JW, Rizen M, Baluk P, Haskell A, Murphy TJ, et al. Cationic liposomes target angiogenic endothelial cells in tumors and chronic inflammation in mice. J Clin Invest. 1998; 101(7):1401–1413. [PubMed: 9525983]
34. Campbell RB, Fukumura D, Brown EB, Mazzola LM, Izumi Y, Jain RK, et al. Cationic charge determines the distribution of liposomes between the vascular and extravascular compartments of tumors. Cancer Res. 2002; 62(23):6831–6836. [PubMed: 12460895]
35. Stephens FO. Induction chemotherapy: to downgrade aggressive cancers to improve curability by surgery and/or radiotherapy. European journal of surgical oncology : the journal of the European Society of Surgical Oncology and the British Association of Surgical Oncology. 2001; 27(7):672–688.
36. Stephens FO. Induction (neo-adjuvant) chemotherapy: systemic and arterial delivery techniques and their clinical applications. The Australian and New Zealand journal of surgery. 1995; 65(10): 699–707. [PubMed: 7487707]
37. Szachowicz-Petelska B, Sulkowski S, Figaszewski ZA. Altered membrane free unsaturated fatty acid composition in human colorectal cancer tissue. Molecular and cellular biochemistry. 2007; 294(1–2):237–242. [PubMed: 16858511]
38. Cooper I, Sasson K, Teichberg VI, Schnaider-Beeri M, Fridkin M, Shechter Y. Peptide derived from HIV-1 TAT protein destabilizes a monolayer of endothelial cells in an in vitro model of the blood-brain barrier and allows permeation of high molecular weight proteins. The Journal of biological chemistry. 2012; 287(53):44676–44683. [PubMed: 23150670]

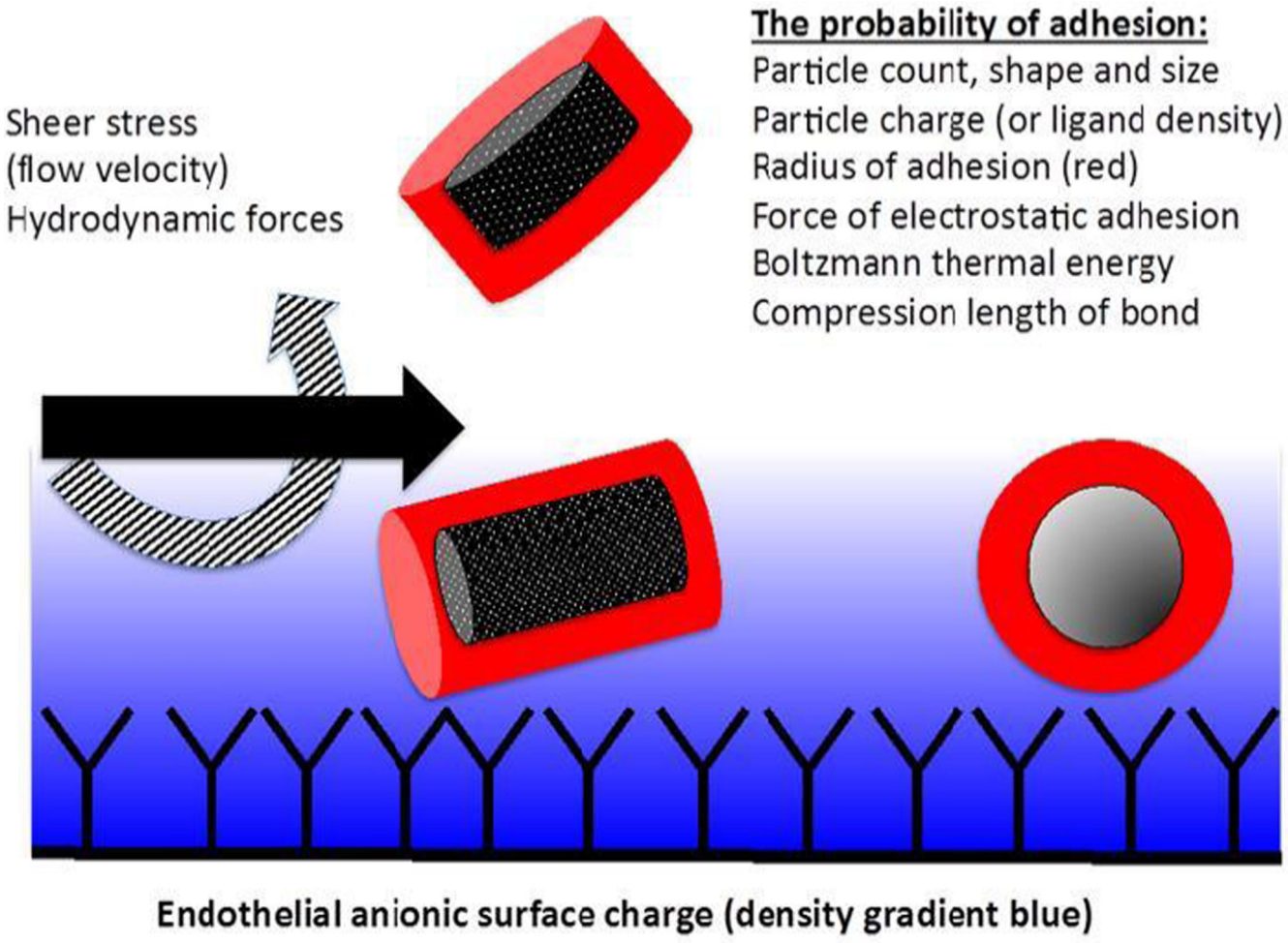

Figure 1. Factors affecting the delivery of nanoparticles

A schematic of the cerebral capillary lumen is shown. Shear stress and hydrodynamic forces tend to displace nanoparticles from the endothelium. Nanoparticle properties including shape, size, and charge as well as ligand-receptor interactions determine the affinity of the particles to attach to the endothelium.

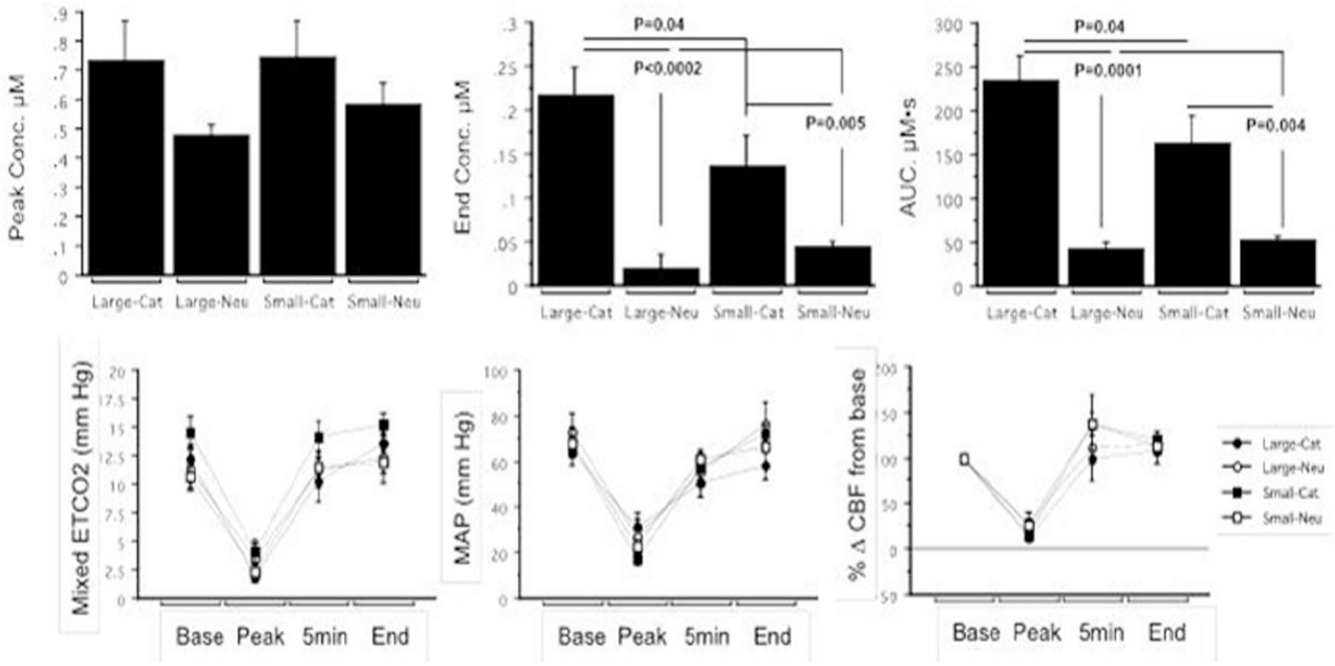

Figure 2. Hemodynamic changes and liposome delivery after intraarterial injection during transient cerebral hypoperfusion in healthy animals

In vivo measurements of liposome delivery to the ipsilateral hemisphere show that both the end concentration and total tissue exposure (AUC) were significantly highest for large cationic liposomes (top panel). Physiological/hemodynamic changes in the animals including end tidal carbon dioxide (ETCO2), mean arterial pressure (MAP), and percent change in cerebral blood flow (CBF) were not significantly dependent on the size or charge characteristics of the liposome delivered (bottom panel).

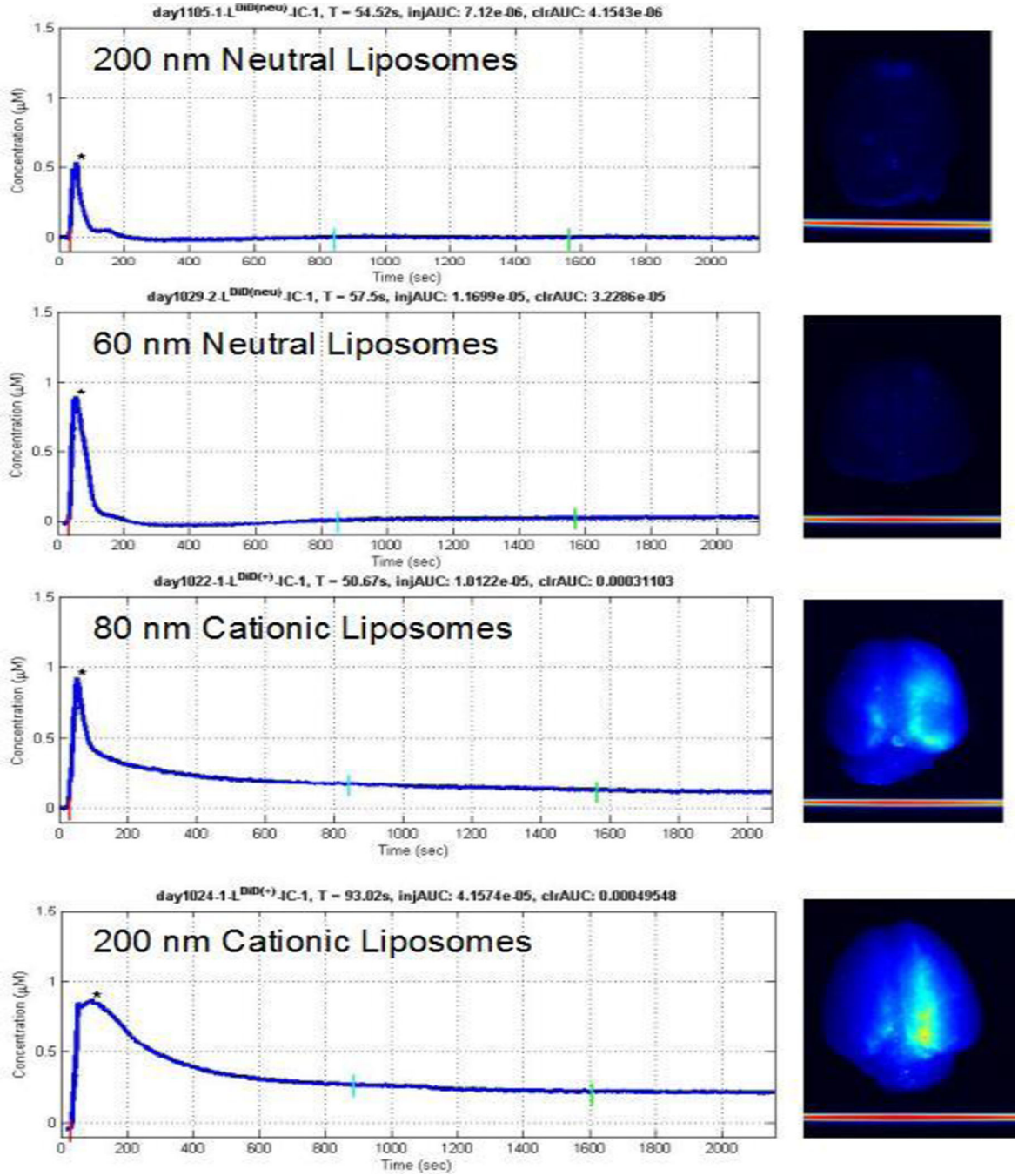

Figure 3. Dynamics of brain liposomal uptake in healthy rats

Concentration-time curves show the real-time, in vivo uptake of liposomes after ipsilateral carotid artery injection (left panel). Multispectral images (MSI) of harvested brain show the degree of liposome deposition for the four liposome types tested (right panel). Note that only minimal neutral liposome deposition is observed on post mortem MSI. Higher intensity MSI signal is evident after 200 nm cationic liposome delivery than after 80 nm cationic liposome delivery.

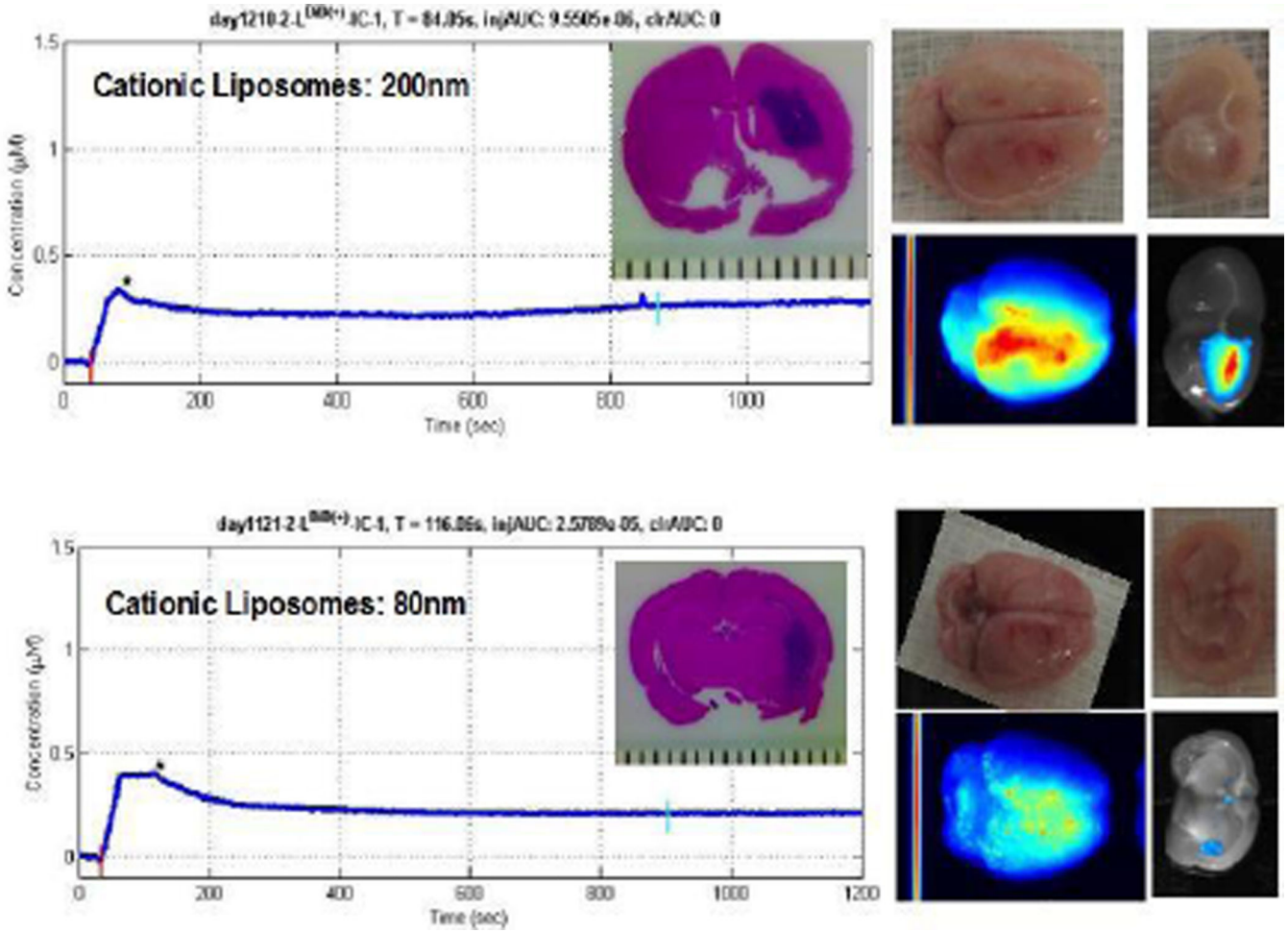

Figure 4. Cationic liposomes specifically target tumor site

Concentration-time curves (left panel) as well as post-mortem multispectral imaging (MSI) of intact glioma-bearing brains (middle panel) indicate that hemispheric delivery of both large and small cationic liposomes occurs after intraarterial delivery. MSI of brain cross-sections (right panel) show that the site of glioma growth is specifically targeted by cationic liposomes. Hematoxylin-eosin stained section through tumor core is also shown (inset, left panel).

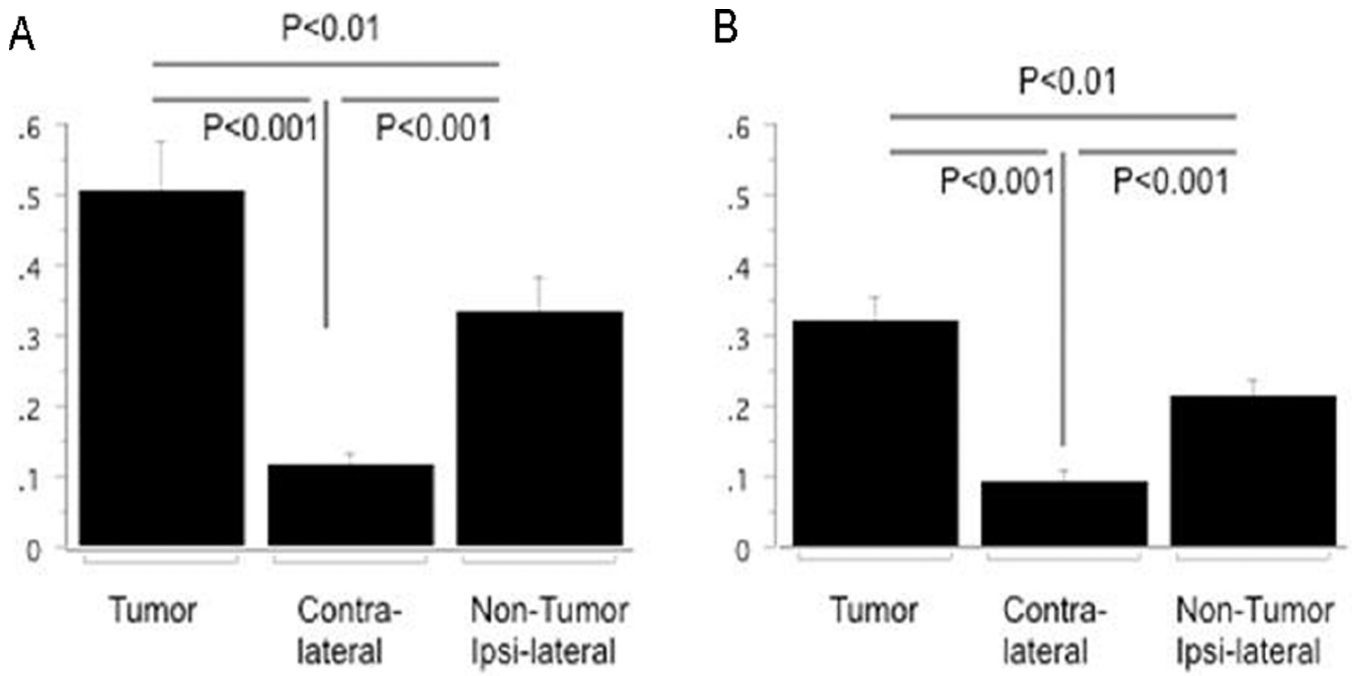

Figure 5. Delivery efficiency of liposomes to gliomas is size dependent

Bar graphs of tissue concentration after 200 nm (A) and 80 nm (B) liposome delivery are shown. Liposome concentrations were significantly greater in the tumor-bearing region as compared to the contralateral hemisphere and the ipsilateral non-tumor brain tissue for both liposomes sizes. Tumor-bearing regions and ipsilateral non-tumor brain tissue had higher concentrations of 200 nm liposomes as compared to 80 nm liposomes ($p=0.03$, each).

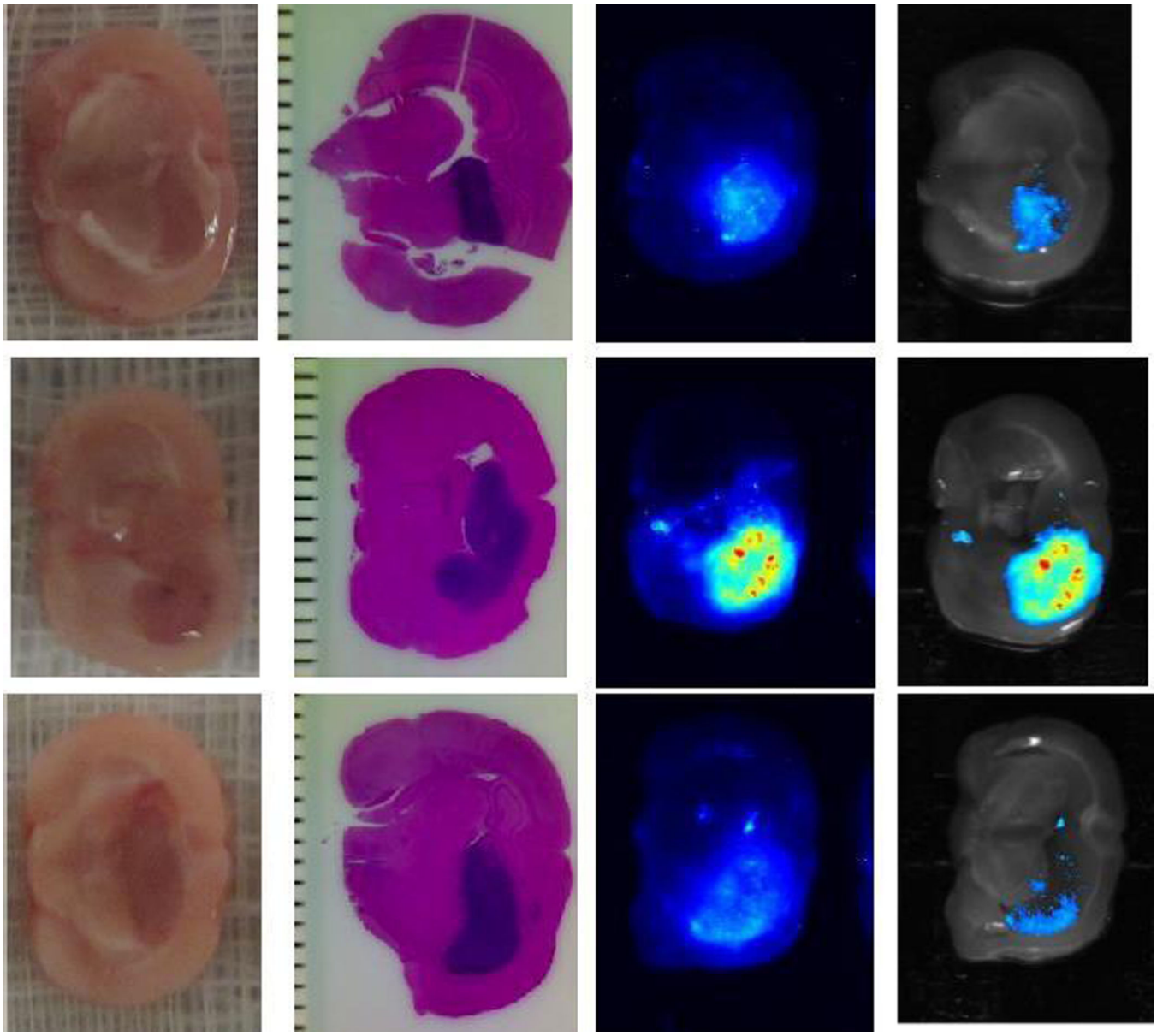

Figure 6. Liposome deposition pattern is variable after intraarterial injection

A diffuse pattern of 200 nm cationic liposome deposition is demonstrated (top panel). Alternatively, incomplete core deposition with regions of dense peripheral deposition could also be seen in larger tumors (middle panel). Even less robust tumor core penetration by 80 nm cationic liposomes is seen in another representative tumor, consistent with 80 nm liposomes being less efficient delivery vehicles than 200 nm liposomes (bottom panel). From left to right: gross section through tumor core, corresponding hematoxylin-eosin stained paraffin section, MSI fluorescence image of liposome deposits, and fluorescence image superimposed on gross section.